

05,13

Influence of thermoinduced magnetoelastic effect on domain structure of planar Ni microparticles

© N.I. Nurgazizov¹, D.A. Bizyaev¹, A.A. Bukharaev¹, A.P. Chuklanov¹, V.Ya. Shur², A.R. Akhmatkhanov²

¹Zavoisky Physical-Technical Institute, FRC Kazan Scientific Center of RAS, Kazan, Russia

²Institute of Natural Sciences and Mathematics, Ural Federal University named after the First President of Russia B.N. Yeltsin, Yekaterinburg, Russia

E-mail: niavn@mail.ru

Received April 29, 2022

Revised April 29, 2022

Accepted May 12, 2022

Results of studying the domain structure of planar Ni microparticles formed on single-crystal substrates from the lithium niobate and from the potassium titanyl phosphate at different temperatures are presented. The dependence of domain sizes on the sample temperature was studied. It is shown the observed change of the domain structure is caused by the magnetoelastic effect, which arises due to the difference in the thermal expansion coefficients of the substrate and microparticles as the sample temperature changes. It is shown, the sizes of magnetic domains, up to the creation of a state with a quasi-homogeneous magnetization may be set by the substrate temperature during the microparticles formation.

Keywords: magnetoelastic effect, magnetic force microscopy, remagnetization, lithium niobate, potassium titanyl phosphate, temperature.

DOI: 10.21883/PSS.2022.09.54171.29HH

1. Introduction

One possible way to change magnetic properties may be to use a magnetoelastic effect (Villari effect) at which a magnetic anisotropy is obtained by means of single-axis mechanical stress in a magnetic medium. The use of such an approach to change the magnetization direction of micro- and nanoparticles is considered to be the most promising at present. If a single particle acts as a medium to record the bit of information, the theoretical estimates suggest that dissipated energy losses can be reduced by several orders compared to the traditional record of information by an external magnetic field [1–5]. The direction of research, when mechanical stresses are used to control the magnetic properties of micro- and nanoobjects, is called Straintronics [1,4].

Different methods can be used to generate mechanical stresses in micro- and nanostructures. One of the most promising methods of creating single-axis mechanical stresses in planar particles is the use of substrates made of piezoelectric materials, the linear dimensions of which can be controlled by the electric field [4–7]. However, other methods are often used to conduct exploratory analysis, for example, mechanical action on a substrate with magnetic structures formed on it [8]. Mechanical stresses can also be generated by changing the sample temperature [9,10]. In this case, the phase transition of the substrate material or the use of the difference in thermal expansion coefficients between the substrate and the structures formed on the substrate may be the determining factor for the mechanical

stresses to be generated. The last variant of substrates may be interesting to make test structures, as it allows a smooth change of the mechanical stress acting on the magnetic structure due to a smooth temperature change. In addition, by forming microparticles on the surface of the substrate at a temperature different from that at which further analysis will be conducted, it is possible to determine in advance the value of the applying to mechanical stress in them.

In the present work, the analysis of the domain structure of planar Ni microparticles of square shape, which had a lateral size of $7.5\mu\text{m}$ and a height of $0.03\mu\text{m}$, were conducted. The microparticles formed on the surface of monocrystalline substrates from congruent lithium niobate LiNbO_3 (CLN) and potassium titanyl phosphate KTiOPO_4 (KTP) at temperatures from room to 80°C . Methods of magnetic force microscopy (MFM) and computer simulation were used for the analysis.

2. Sampling and analysis methodology

Monocrystalline substrates with optical polished surface (Crystal Technology Inc.) were used to make microparticles. The CLN substrates were cut out in such a way that the crystal axis c and its perpendicular axis a lay in the plane on which the microparticles formed. The size of these substrates was $9 \times 3 \times 1\text{ mm}$. At the same time, the axis c was directed along the long side of the substrate, which allowed it to be oriented during deposition and measurement. According to the manufacturer, the temperature coefficient of linear expansion

of CLN along the axis a $\alpha_1 = 15 \cdot 10^{-6} \text{ K}^{-1}$, along the axis c $\alpha_3 = 7.5 \cdot 10^{-6} \text{ K}^{-1}$. Thus the expansion of the crystal when heated along the axis a is 2 times larger than along the axis c . KTP substrates were cut out so that the crystallographic axes Y and Z lay in the particle-forming plane, the thermal expansion coefficients along which were $\alpha_y = 9 \cdot 10^{-6} \text{ K}^{-1}$ and $\alpha_z = 0.6 \cdot 10^{-6} \text{ K}^{-1}$. The dimensions of these substrates were $10 \times 4 \times 1 \text{ mm}$ and the long side was directed along the axis Y .

Arrays of square-shaped planar nickel microparticles were formed on the surface of substrates by electron beam evaporation of solid under ultrahigh vacuum conditions. The deposition was carried out through a metal mesh with identical square holes pressed to the surface. In one sputtering cycle two samples were produced on the substrates of the first and second types. Four batches of samples were produced at temperatures: 32, 45, 60 and 80°C, which allowed changing the direction of the magnetoelastic anisotropy induced in microparticles by heating or cooling the sample relative to the deposition temperature. After the formation of the microparticles, the mesh was removed and a solid Ni film of 3 nm thickness was deposited onto the sample surface at the same temperatures to neutralize the electrostatic interaction of the MFM probe with the sample. During measurements, the film and the MFM probe were grounded. The film was deposited at parameters similar to the deposition of microparticles in order to have the same temperature coefficients of linear expansion. The use of other conductive films to neutralize the charge of the crystal could result in additional mechanical stresses in the microparticles at the change of temperature.

The distance between the sides of the adjacent $5.2 \mu\text{m}$ particles made it possible to eliminate the influence of the magnetic structure of one particle on the adjacent particles. The formed array of microparticles covered an area of about 4 mm^2 , allowing MFM analysis to select the required microparticle ensemble. The resulting Ni microparticles had a polycrystalline structure and a linear expansion ratio of $13 \cdot 10^{-6} \text{ K}^{-1}$ [11]. The saturation magnetostriction constant of (λ_s) microparticles had a negative sign and was equal to $-37 \cdot 10^{-6}$ [12].

The ratio of linear expansion coefficients of microparticles and the substrate should have caused the CLN substrates to heat the sample above the sputtering temperature, causing mainly microparticle compression along the c axis of the crystalline substrate and their slight expansion along the a axis (Fig. 1, *a*). Due to the negative sign of magnetostriction this will lead to the formation Easy Magnetization Axis of microparticles along the c axis of the substrate. When the sample is cooled below the deposition temperature, the microparticle will be mostly stretched along the c axis and slightly compressed along the a axis, resulting in the formation of Easy Magnetization Axis of microparticles along the a axis. At the same time, both compression and stretching of the microparticle on CLN substrates will lead to guiding of magnetic anisotropy in one direction.

When the microparticles are heated on the KTP substrate above the deposition temperature, there should be

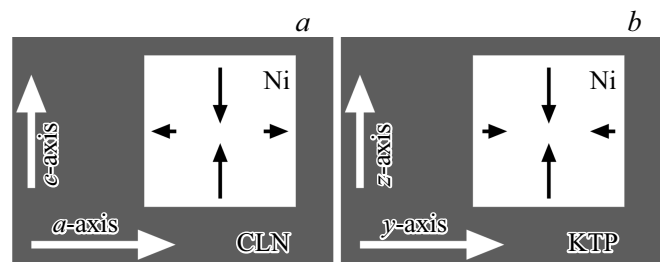


Figure 1. The Ni microparticles arrangement scheme on substrates CLN (*a*) and KTP (*b*) and the forces applied to it when the sample is heated above the particle forming temperature.

mainly a compression of microparticles along z axis of the crystalline substrate and their slight compression along the y axis (Fig. 1, *b*). This leads to the formation of Easy Magnetization Axis along the z , axis, while compression along the y axis weakens the induced uniaxial anisotropy. When the sample is cooled below the spray temperature, the microparticle will be mostly stretched along the z axis and slightly compressed along the y axis, resulting in the formation of an axis of light magnetization of microparticles along the y axis.

To study the geometric parameters and magnetization distribution in microparticles, a scanning probe microscope (SPM) Solver P47 (NT MDT) was used, additionally equipped with an electromagnet and thermo-cell. This was allowed to perform MFM measurements in constant in-plane magnetic field of up to $\pm 16 \text{ mT}$ with simultaneous heating the sample up to 110°C. MFM measurements were carried out using a single-pass method (when the probe is at a constant distance from the examined surface during scanning) in order to reduce the possible influence of the probe on the magnetization distribution in microparticles. Magnetic cantilevers Multi75M-G (BudgetSensor) and PPP-LM-MCMR (Nanosensor) were used.

3. Experimental results and discussion

Atomic-force microscopy (AFM) of the obtained samples showed that the formed microparticles have good repeatability of shape and size on the whole occupied area (Fig. 2, *a*). The particle sizes were $7.5 \times 7.5 \times 0.03 \mu\text{m}^3$. The edge defects of some microparticles did not have a noticeable influence on the MFM image (Fig. 2).

The analysis on the magnetic structure of Ni microparticles that were formed without additional heating substrates showed that at room temperature, the domain structure consists of four domains of approximately the same size, the direction of magnetization in which is parallel to the side at which the domain is located (Fig. 2, *b*). This is the so-called Landau structure, which is characteristic of square planar particles that are not affected by mechanical stress and external magnetic field. An increase in the temperature of the sample leads to a mechanical stress in the microparticles and a change in the domain structure.

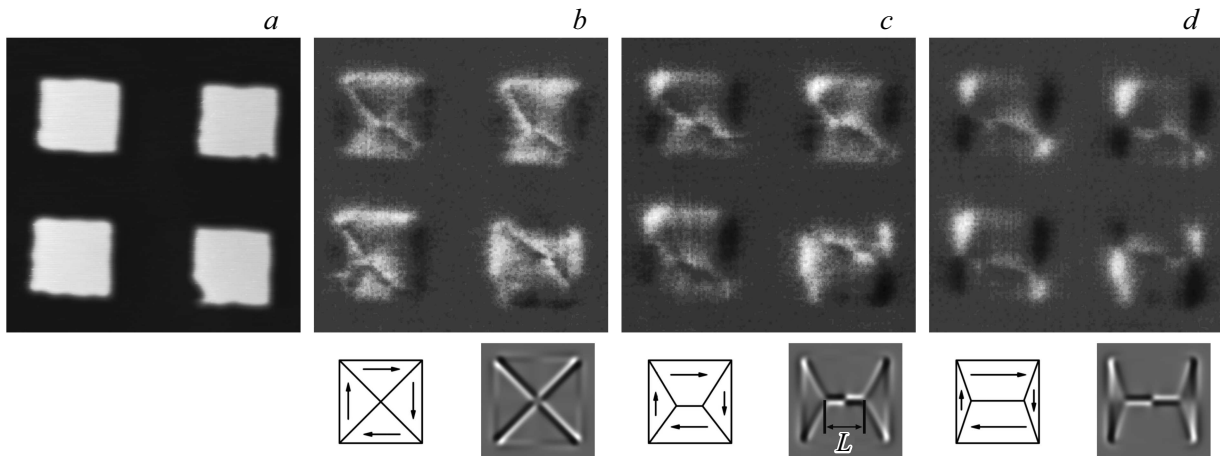


Figure 2. AFM image of Ni microparticles — (a) formed at room temperature on the CLN substrate and corresponding MFM images of these microparticles obtained at room temperature — (b), 40°C — (c), 60°C — (d). Below each MFM image is a schematic representation of the magnetization distribution in the microparticle, modeled by OOMMF, and the corresponding virtual MFM image. The scanning field is $23 \times 23 \mu\text{m}^2$. The height scale on AFM image (a), corresponding to grayscale is 35 nm. The phase span for MFM images corresponding to grayscale is 1° . L — length of the domain wall between the two domains increased by magnetically induced anisotropy.

By compressing the particle in the direction of the c axis for CLN substrates or z axis for KTP substrates and negative microparticle magnetostriction, the domains whose magnetization direction is directed along these axes (Fig. 2, c) increase. Between these domains, a domain wall is formed, the length (L) of which is proportional to the size of the enlarged domains, and which can be used to characterize the effect of the mechanical stress particle [8]. With the increase of sample temperature, this domain wall length increases (Fig. 2, d).

Samples formed at temperatures above the room temperature had a four-domain structure. The two domains were enlarged in size and had a distinctive domain wall between them. In microparticles on the CLN substrates, the direction of magnetization in these domains was perpendicular to the axis c , which indicates that the particles were stretched in this direction (Fig. 3, a). In microparticles on the KTP substrates the domains perpendicular to the z axis increased, which indicates that the particles were stretched in this direction.

In the sample on the CLN substrate formed at 80°C, some microparticles at room temperature were in a quasi-uniform magnetized state (Fig. 3, a). The increase in the temperature of the sample results in the formation of a four-domain structure in such microparticles and an overall reduction in the size of the two large original domains in all the microparticles (Fig. 3, b). At a temperature close to the temperature of the formation of microparticles, domain sizes become approximately the same (Fig. 3, c), indicating that the thermoinduced uniaxial mechanical stress in the microparticle tends to zero and stops affecting the domain structure. Further temperature increase increases the size of the domains, the magnetization of which is directed along the axis c for CLN substrates and along the axis z for KTP substrates.

To characterize the changes observed in the domain structure of microparticles, the domain wall length of L formed between the two enlarged domains was measured. The ratio of the domain wall length to microparticle size in this direction was averaged at 9 microparticles from a single MFM scan. The measurement results are presented in Fig. 4. Measurements were made in increments of 5°C , with the sample heated at no more than 40°C relative to the temperature at which the microparticles formed. It was found that in this case, repeated cycles of heating and cooling of the sample return the domain structure of the microparticle to its original state. With heating by more than 40°C , the domain structure of the microparticles after cooling to room temperature may not have returned to its original state.

In general, based on the MFM image obtained, it is impossible to unequivocally restore the magnetization distribution in the object under study. In MFM measurements, a signal proportional to the phase difference between the signal causing the magnetic probe to oscillate at the resonance frequency and the signal characterizing these oscillations is recorded. This signal is proportional to the gradient of the interaction force of the probe with the magnetic field of the sample at a given point [13]. The following approach is used to visualize the magnetization distribution. On the basis of data on the shape and size of the object, and parameters characterizing its magnetic properties (constant of exchange interaction, magnetization of saturation, crystal anisotropy, etc.), such distribution of local magnetic moments is calculated, at which it has minimal magnetic energy. The MFM image is then modelled on the basis of this distribution and compared with the experimental image. When these images coincide, it is concluded that the model magnetization distribution

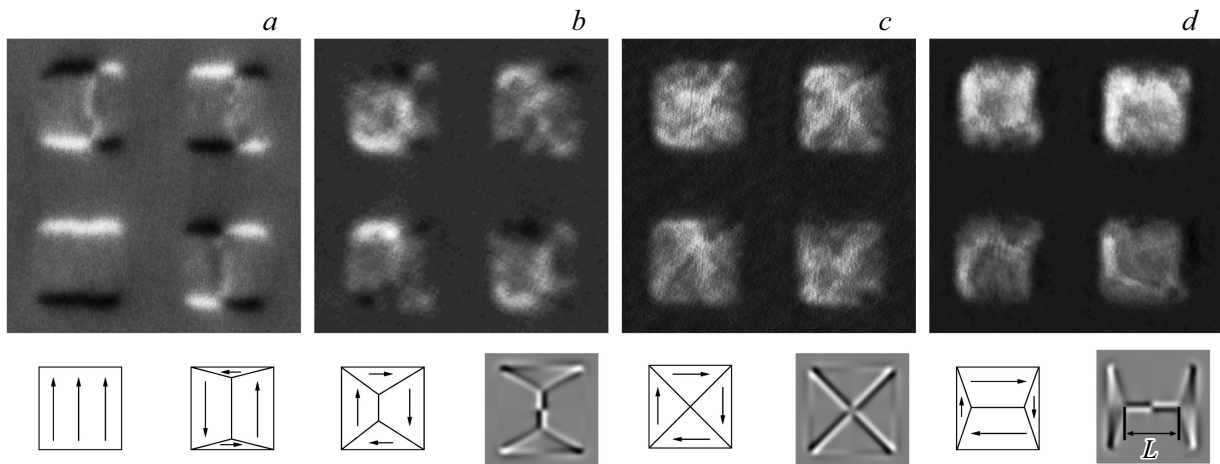


Figure 3. MFM images of Ni microparticles formed on a CLN substrate at a temperature of 80°C obtained at (a) room temperature, (b) 70°C, (c) 80°C, (d) 100°C. Under the MFM image (a) are only the magnetization distribution schemes in the microparticles (quasi-homogeneous magnetization for the lower left particle and quadruple magnetization for the rest). Below each MFM image is a schematic representation of the magnetization distribution in the microparticle, modeled by OOMMF, and the corresponding virtual MFM image. The scanning field is $23 \times 23 \mu\text{m}^2$. The phase span for MFM images corresponding to grayscales is 1° . L — length of the domain wall between the two domains increased by magnetoelastic anisotropy.

corresponds to the real one. If the images do not match, one of the parameters on which the simulation is based will vary.

The OOMMF [14] software was used to model the magnetic structure of the particle, and a virtual MFM image was calculated based on the obtained magnetization distribution. The software Virtual MFM [15], which was developed earlier, allows to take into account the geometric parameters of the probe and the height of its movement over the analyzed structure. Under OOMMF modeling, the saturation magnetization of Ni was assumed to be 490 kA/m, while the exchange rate constant was assumed to be equal to $9 \cdot 10^{-12} \text{ J/m}^3$ [14]. The influence of magnetoelastic effect on magnetization distribution was considered by the introduction of the uniaxial anisotropy constant (K_{eff}), which increased from 0 to 5000 J/m^3 with the increment of 100 J/m^3 . The direction of anisotropy in the simulation was determined by the parallel side of the microparticle. With $K_{\text{eff}} = 0$ in the microparticle, four domains of the same size were observed with the direction of magnetization parallel to the side of the microparticle near which it is located (Fig. 2, b). The virtual MFM image modeled on this distribution is well consistent with the experimental ones (Figure. 2, b, 3, c). At $K_{\text{eff}} > 300 \text{ J/m}^3$ the domains size increase begins, the magnetization direction of which coincides with the anisotropy direction (Fig. 2, c, d). In this case, a characteristic bridge is formed between the two domains, similar to that observed in experimental images. The K_{eff} value can be converted to mechanical stress (σ), applied to a microparticle, based on the formula: $\sigma = -2/3 \cdot K_{\text{eff}}/\lambda_s$, where λ_s — is the constant of saturation magnetostriction of the material used.

Based on the difference in the temperature expansion coefficients of the substrate and the microparticles on different axes, it is possible to estimate the uniaxial mechanical

stress at the sample temperature change. The change of the particle size (Δl) along the selected axis provided that it is inextricably linked to the substrate will be

$$\Delta l = \Delta T \cdot L \cdot \alpha, \quad (1)$$

where ΔT — temperature change, L — original particle size along the selected axis (in this case it is the side of the square particle, as the particles are oriented by their sides along the axis of the crystal), α — uniaxial particle thermal expansion coefficient relative to the substrate, which is equal to

$$\alpha = (\alpha_1 - \alpha_p) - (\alpha_2 - \alpha_p) = \alpha_1 - \alpha_2, \quad (2)$$

where α_p — microparticle thermal expansion coefficient (in our case the microparticle is polycrystalline, and it is the same for all directions $-13 \cdot 10^{-6} \text{ K}^{-1}$), α_1 and α_2 — linear coefficients of thermal expansion of the substrate along the crystallographic axes that form the surface on which the microparticles are formed. For CLN substrates, the axes are a ($\alpha_1 = 15 \cdot 10^{-6} \text{ K}^{-1}$) and c ($\alpha_2 = 7.5 \cdot 10^{-6} \text{ K}^{-1}$), respectively $\alpha = 7.5 \cdot 10^{-6} \text{ K}^{-1}$. For KTP substrates, these axes are y ($\alpha_1 = 9 \cdot 10^{-6} \text{ K}^{-1}$) and z ($\alpha_2 = 0.6 \cdot 10^{-6} \text{ K}^{-1}$), respectively $\alpha = 8.4 \cdot 10^{-6} \text{ K}^{-1}$. If one accepts that the mechanical stress (σ) applied to the microparticle is: $\sigma = Y \cdot \varepsilon$, where Y is the Jung module of the material from which the microparticle is made, ε — the deformation (or the uniaxial size change) of the microparticle ($\varepsilon = \Delta l/L$), then the dependence of the induced stress upon temperature change will be equal to

$$\sigma = Y \cdot \Delta T \cdot \alpha. \quad (3)$$

Thus, on the basis of the obtained experimental temperature dependence of the domain wall length, it is possible to

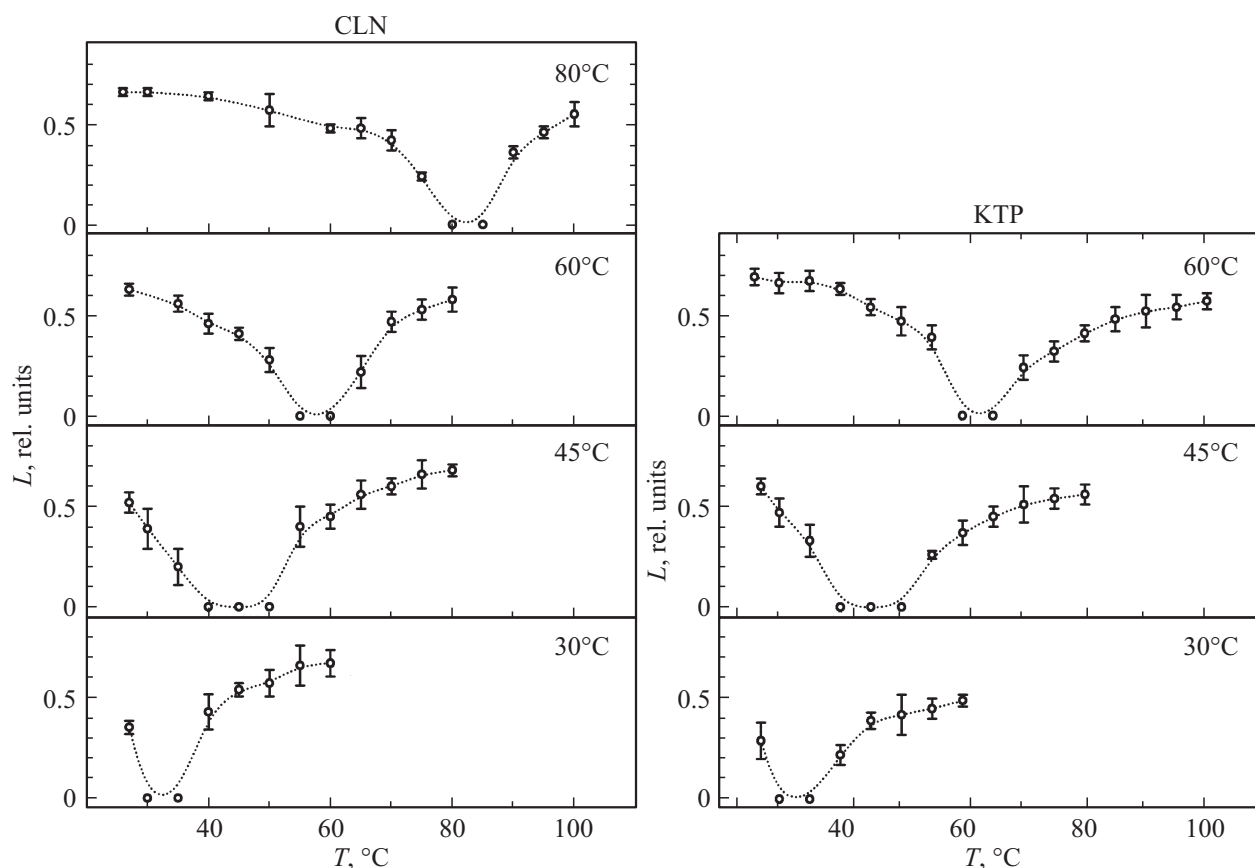


Figure 4. Experimental dependences of domain wall L length to sample temperature for microparticles formed at different temperatures (shown in the graph) on CLN and KTP substrates.

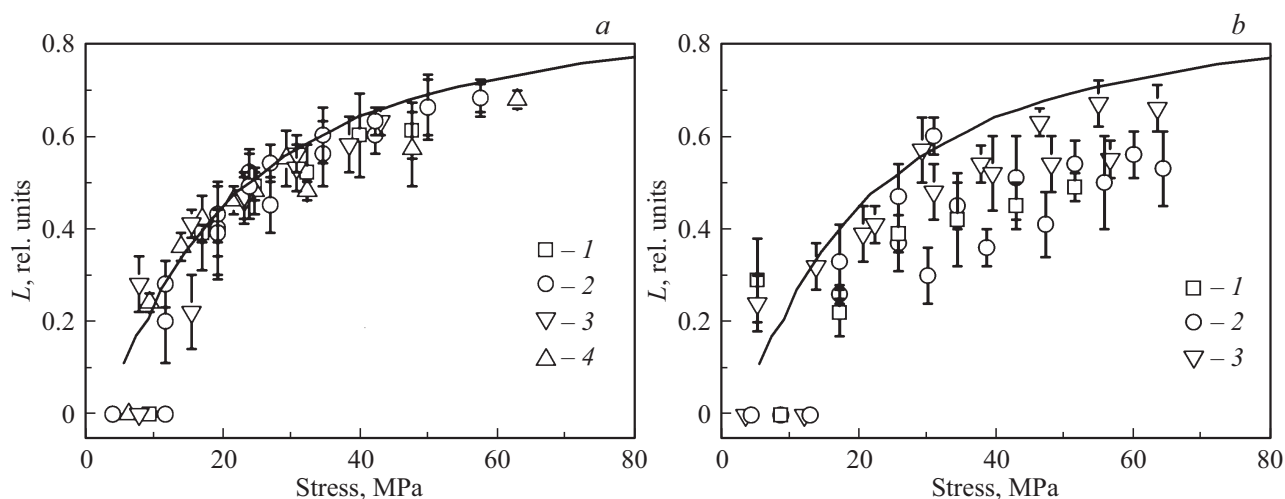


Figure 5. The domain wall length L depends on the uniaxial mechanical stress for the particles generated at CLN — (a) and KTP — (b) substrates at different temperatures. The figures are the data obtained for microparticles generated: 1 — at room temperature, 2 — at 45°C, 3 — at a temperature of 60°C and 4 — at a temperature of 80°C. Solid line is the result of domain wall length simulation with OOMMF.

calculate the dependence of the bridge length on mechanical stress and to compare it with the calculations made with OOMMF (Fig. 5). For calculations, the value of the Young module for Ni microparticles was assumed to be 210 GPa according to work [11].

The experimental and theoretical dependences given for microparticles, formed on CLN substrates are quite well matched. In the case of KTP substrates, there is a wide range of experimental data and their divergence from theoretical calculations. We suspect this may be due to

poor adhesion of Ni microparticles to the surface of KTP crystal. In this case, the thermal expansion of the substrate is not fully transmitted to the microparticle and its mechanical stresses are less than the theoretically calculated ones. This leads to the conclusion that CLN substrates are more promising for creating test magnetic microstructures, despite a slightly lower temperature expansion rate than of KTP substrates. As studies have shown on CLN substrates, it is possible to create microparticles with predetermined domain sizes at room temperature by changing the temperature of the substrate on which they are deposited, and in the future effectively vary these sizes, by changing the temperature of the sample.

4. Conclusion

Studies have shown that anisotropic thermal expansion of a monocrystalline substrate affects the domain structure applied to it by planar Ni microparticles. Thus, at room temperature it is possible to obtain the necessary domain structure of particles by forming microparticles at a given temperature. It has been shown that substrates from congruent lithium niobate are more promising because they allow to produce a higher thermoinduced magnetic anisotropy in microparticles. It has been determined that for replicable domain structure management of Ni microparticles with the sizes of $7.5 \times 7.5 \times 0.03 \mu\text{m}^3$, a range of single-axis mechanical stress up to 60 MPa is sufficient. Stresses above 60 MPa can result in a quasi-homogeneous magnetization state in the microparticle.

Funding

This work was supported by grants from the RSF (project № 22-29-00352).

Conflict of interest

The authors declare that they have no conflict of interest.

References

- [1] K. Roy, S. Bandyopadhyay, J. Atulasimha. *Appl. Phys. Lett.* **99**, 63108 (2011).
- [2] M. Barangi, P. Mazumder. *IEEE Nanotechnol. Mag.* **9**, 3, 15 (2015).
- [3] J. Atulasimha, S. Bandyopadhyay. *Nanomagnetic and Spintronic Devices for Energy-Efficient Memory and Computing.* WILEY (2016). 352 c.
- [4] A.A.A. Bukharaev, A.K. Zvezdin, A.P. Pyatakov, Yu.K. Fetisov. *Phys. Usp.* **61**, 1175 (2018).
- [5] S. Bandyopadhyay, J. Atulasimha, A. Barman. *Appl. Phys. Rev.* **8**, 041323 (2021).
- [6] S. Finizio, M. Foerster, M. Buzzi, B. Kruger, M. Jourdan, C.A.F. Vaz, J. Hockel, T. Miyawaki, A. Tkach, S. Valencia, F. Kronast, G.P. Carman, F. Nolting, M. Klau. *Phys. Rev. Appl.* **1**, 021001 (2014).
- [7] A. Chen, Y. Zhao, Y. Wen, L. Pan, P. Li, X. Zhang. *Sci. Adv.* **5**, 12, eaay5141 (2019).
- [8] I. Nurgazizov, D.A. Bizyaev, A.A. Bukharaev, A.P. Chuklanov. *Phys. Solid State* **62**, 1667 (2020).
- [9] D.A. Bizyaev, A.A. Bukharaev, N.I. Nurgazizov, A.P. Chuklanov, S.A. Migachev. *Phys. Status Solidi Rapid Res. Lett.* 2000256 (2020).
- [10] N.I. Nurgazizov, D.A. Bizyaev, A.A. Bukharaev, A.P. Chuklanov, V.Ya. Shur, A.R. Akhmatkhanov. *Phys. Solid State* **63**, 1427 (2021).
- [11] A.P. Babichev, N.A. Babushkina, A.M. Bratkovsky and others. *Physical quantities: Handbook / Ed. by I.S. Grigoriyev, Ye.Z. Meylikhov.* Energoatomizdat, M. (1991), 1232 p. (in Russian).
- [12] K.P. Belov. *Magnitostriksionniye yavleniya i ikh tekhnicheskkiye prilozheniya.* Nauka, M. (1987). 160 s. (in Russian).
- [13] U. Hartmann. *Annu. Rev. Mater. Sci.* **29**, 53 (1999).
- [14] M.J. Donahue, D.G. Porter. *OOMMF User's Guide, Version 1.0.* Natl. Inst. Standards Technol., Gaithersburg, MD, USA (1999). <http://math.nist.gov/oommf>.
- [15] D.V. Ovchinnikov, A.A. Bukharayev. *Tech. Phys.* **46**, 1014 (2001).